Quantum Information and Computation, Vol. 11, No. 7&8 (2011) 0592–0605

OPTIMAL DETERMINISTIC ENTANGLEMENT CONCENTRATION OF POLARIZED PHOTONS THROUGH DIRECT SUM EXTENSION AND CAVITY-ASSISTED INTERACTION

WEN-DONG LI, WEN-ZHAO ZHANG, LI-ZHEN MA, YONG-JIAN GU[a]
Department of Physics, Ocean University of China,
Qingdao 266100, People's Republic of China

Received July 8, 2010
Revised May 3, 2011

A scheme for optimal deterministic entanglement concentration is proposed, and its corresponding optical realization based on a cavity-assisted linear optical system is presented. In this scheme, the quantum circuit devised is simpler than that built in [Y. J. Gu, et al. (2006), Phys. Rev. A. 73, 022321], as it requires the minimum ancillary dimensions and the number of unitary operations. Moreover, we show that, by introducing a path-polarization entanglement state based on the direct sum extension method, three elementary controlled phase-flip gates between two photons are sufficient in the design of its optical realization scheme, making it easy to be implemented from the experimental point of view. Meanwhile, the scheme is verified effective to recover highly entangled pairs from mixed states.

Keywords: entanglement concentration, direct sum extension, optical realization, path-polarization entanglement state
Communicated by: R Jozsa & G Milburn

1 Introduction

The high-quality entanglement is an indispensable resource in quantum information processing including quantum communication [1, 2, 3, 4] and quantum computation [5]. However this resource is very fragile; its quality is easily degraded by decoherence and dissipation processes during the interaction with the environment, especially considering that the interaction is unavoidable because the distribution of entangled particles is necessary in some schemes. This detrimental effect has prompted the development of entanglement distillation and concentration protocols [6, 7, 8, 9, 10, 11, 12, 13, 14, 15, 16], which aim to recover highly entangled pairs from mixed or nonmaximally entangled pairs.

So far, not all of those protocols can be easily realized experimentally; moreover, the success probability of them being realized is also very low [17, 18, 19, 20, 21, 22, 23, 24]. Considering to reduce the failing risk of experimental realization, the deterministic entanglement concentration (DEC) protocol [25, 26] and its implementation scheme in atomic system [27] have been developed recently. This protocol can deterministically (without gambling) extract a maximally entangled Einstein-Podolsky-Rosen (EPR) pair shared by two distant people from two partially entangled pairs under certain conditions theoretically, but this procedure

[a]yjgu@ouc.edu.cn

is difficult to be implemented in an experiment because there exist too many operations on qubits.

In this paper we first propose a protocol of DEC, and then design an experimental scheme in optical systems. In the protocol, a unitary operation used to perform a positive operator-valued measure (POVM) is constructed in an optimal way, in which the number of ancillary dimensions used is minimum, as have been proved by Chen et al. [28]. Unlike the protocol in Ref. [26] that extends the Hilbert space by introducing two ancillary qubits, this protocol employs two extra dimensions or degrees of freedom of the original system. The latter requires fewer operations when realized as quantum circuits. Based on the direct sum extension method [28, 29], several paths of a single photon are encoded as the quantum states to extend the Hilbert space in the experimental scheme. This further reduces the number of controlled operations between two photons and only three of them are needed in the end. The corresponding system is easier to be realized in experiment as fewer steps are required. In addition, the experimental scheme is more valuable in application because photons usually act as 'flying' qubits in the quantum communication.

The paper is organized as follows: in section 2, the DEC protocol is optimally constructed based on the direct sum extension space, and its corresponding quantum circuit is presented. In section 3, we propose an optical realization scheme for implementing the protocol in linear optical systems with the cavity-assisted interaction. It is shown that three elementary controlled phase-flip gates between two photons are sufficient for the scheme. In section 4, the DEC protocol is performed on a particular type of mixed states, and its effectiveness is analyzed. We conclude the paper in Section 5 with a brief summary.

2 Optimal deterministic entanglement concentration protocol

The DEC protocol deterministically extracts an EPR pair from two partially entangled pairs AB and $A'B'$, in which particles A, A' and B, B' belong to two distant parties Alice and Bob, respectively. The partially entangled state [6, 20, 25] can be generated by experiment [30]. Using the Schmidt decomposition [6, 31, 32], this initial state may be written as

$$\begin{aligned} |\Psi_0\rangle_{AA'BB'} &= |\psi\rangle_{AB} \otimes |\varphi\rangle_{A'B'} \\ &= \left(\sqrt{a}\,|00\rangle_{AB} + \sqrt{1-a}\,|11\rangle_{AB}\right) \otimes \left(\sqrt{b}\,|00\rangle_{A'B'} + \sqrt{1-b}\,|11\rangle_{A'B'}\right), \quad (1) \end{aligned}$$

where the Schmidt coefficients a and b are positive real numbers, and without loss of generality, we can set $1/2 < a \leq b < 1$.

Traditionally, the procedure of extracting an EPR pair state $\left(\left(|00\rangle + |11\rangle\right)/\sqrt{2}\right)$ shared by Alice and Bob includes the following steps [26]. First, Alice executes a local measurement described by a POVM, then one-way classical communication from Alice to Bob is performed, and finally Bob's corresponding local unitary operation or choice between the two pairs is made. According to Neumark's theorem [33], to perform the POVM, we need extend the Hilbert space and construct a unitary operation and then execute an orthogonal measurement. This process is described in detail as following.

On Alice's side, the orthonormal basis of the Hilbert space $H_S = H_A \otimes H_{A'}$ is $\{|j\rangle, j = 0, 1, 2, 3\} \equiv \{|00\rangle_{AA'}, |01\rangle_{AA'}, |10\rangle_{AA'}, |11\rangle_{AA'}\}$. The first step is to expand the space H_A of particle A into $\tilde{H}_A \equiv \{|0\rangle, |1\rangle, |2\rangle, |3\rangle\}$ using the direct sum extension method by introducing two extra dimensions $|2\rangle, |3\rangle$ of particle A. So the space H_S is expanded as $\tilde{H}_S = \tilde{H}_A \otimes H_{A'}$,

the orthonormal basis of which is $\{|k\rangle, k = 1, \cdots, 8\} \equiv \{|00\rangle_{AA'}, |01\rangle_{AA'}, |10\rangle_{AA'}, |11\rangle_{AA'}, |20\rangle_{AA'}, |21\rangle_{AA'}, |30\rangle_{AA'}, |31\rangle_{AA'}\}$.

The next step is to unitarily transform the initial state (1) to the state $|\Psi_m\rangle_{AA'BB'}$, which can be expressed as

$$\begin{aligned} |\Psi_m\rangle_{AA'BB'} &= \sqrt{a(1-b)}\,(|0000\rangle + |0101\rangle) \\ &\quad + \sqrt{(1-2ab)/2}\,(|1010\rangle + |1111\rangle) \\ &\quad + \sqrt{(2a-1)(2b-1)/2}\,(|2000\rangle + |2111\rangle) \\ &\quad + \sqrt{(2b-1)/2}\,(|3000\rangle + |3110\rangle), \end{aligned} \tag{2}$$

where the particles are arranged in the order of $AA'BB'$.

The unitary matrix U is constructed as

$$U = \sum_{k=1}^{8}\sum_{l=1}^{8} u_{k,l}\,|k\rangle\langle l|, \tag{3}$$

where $u_{1,1} = \sqrt{\frac{1-b}{b}}$, $u_{2,2} = 1$, $u_{3,3} = \sqrt{\frac{1-2ab}{2(1-a)b}}$, $u_{4,4} = \sqrt{\frac{1-2ab}{2(1-a)(1-b)}}$, $u_{5,1} = \sqrt{\frac{(2a-1)(2b-1)}{2ab}}$, $u_{6,4} = \sqrt{\frac{(2a-1)(2b-1)}{2(1-a)(1-b)}}$, $u_{7,1} = \sqrt{\frac{2b-1}{2ab}}$, $u_{8,3} = \sqrt{\frac{2b-1}{2(1-a)b}}$, and other elements $u_{k,l}$ in the first four columns of U are equal to 0. Elements from remaining columns can then be constructed to meet the unitary requirement.

An orthogonal measurement is then performed on particle A. For each measurement result j, we obtain the following states

$$\begin{aligned} &\frac{1}{\sqrt{2}}(|00\rangle_{A'B'} + |11\rangle_{A'B'}) \otimes |0\rangle_B, && j = 1, \\ &\frac{1}{\sqrt{2}}(|00\rangle_{A'B'} + |11\rangle_{A'B'}) \otimes |1\rangle_B, && j = 2, \\ &\frac{1}{\sqrt{2}}(|000\rangle_{A'BB'} + |111\rangle_{A'BB'}), && j = 3, \\ &\frac{1}{\sqrt{2}}(|00\rangle_{A'B} + |11\rangle_{A'B}) \otimes |0\rangle_{B'}, && j = 4, \end{aligned} \tag{4}$$

and the corresponding probabilities $\{p_j, j = 1, \cdots, 4\}$ are

$$p_1 = 2a(1-b), p_2 = 1-2ab, p_3 = (2a-1)(2b-1), p_4 = 2b-1. \tag{5}$$

Because probabilities should be non-negative real numbers, the coefficients a and b need to satisfy the condition $ab \leq 1/2$. The condition can also be obtained by Nielsen's theorem [31]. This means that in order to ensure the success of the DEC protocol, the states $|\psi\rangle_{AB}$ and $|\varphi\rangle_{A'B'}$ in Eq. (1) cannot deviate too far from the maximally entangled state simultaneously. It can be seen from Fig. 1, the fidelity F between the initial state $|\Psi_0\rangle_{AA'BB'}$ and the two EPR pairs state $|E\rangle \otimes |E\rangle$ ($|E\rangle = (|00\rangle + |11\rangle)/\sqrt{2}$) can't be too small, as the fidelity represented by red stars (corresponding to $ab \leq 1/2$) is larger than that represented by blue points (corresponding to $ab > 1/2$) for specific values of b.

It is worth noting that linearly independent vectors are formed by eight rows of the first four columns in the unitary matrix U. This means the number of ancillary dimensions used

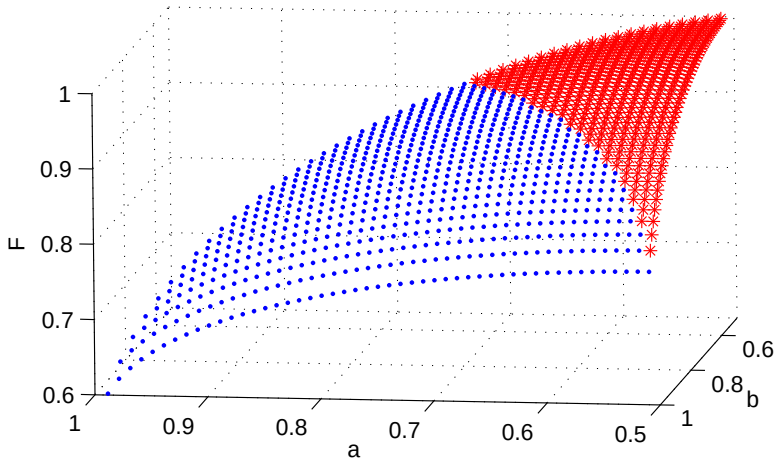

Fig. 1. The fidelity between the initial state and the state of two EPR pairs. Red stars and blue points correspond to $ab \leq 1/2$ and $ab > 1/2$, respectively. a and b satisfy the condition $1/2 < a \leq b < 1$.

here to accomplish the DEC task is minimum [28], securing that the protocol is optimal. Furthermore, the U here contains a small number of controlled operations, only three controlled-U gates and one C-NOT gate. This is also much simpler than the traditional one in Ref. [26], in which seven controlled gates among more than three qubits are contained. The quantum circuit is shown in Fig. 2, in which operators X_a, U_1, U_3, U_4 are defined as

$$X_a = \begin{pmatrix} 1 & 0 & 0 & 0 \\ 0 & 0 & 0 & 1 \\ 0 & 0 & 1 & 0 \\ 0 & 1 & 0 & 0 \end{pmatrix},$$

$$U_1 = \begin{pmatrix} \sqrt{\frac{1-b}{b}} & 0 & \sqrt{\frac{(1-b)(2b-1)}{b(2ab-2b+1)}} & -\sqrt{\frac{(2a-1)(2b-1)}{2ab-2b+1}} \\ 0 & 1 & 0 & 0 \\ \sqrt{\frac{(2a-1)(2b-1)}{2ab}} & 0 & \sqrt{\frac{(2a-1)(2b-1)^2}{2ab(2ab-2b+1)}} & \sqrt{\frac{2a(1-b)}{2ab-2b+1}} \\ \sqrt{\frac{2b-1}{2ab}} & 0 & -\sqrt{\frac{2ab-2b+1}{2ab}} & 0 \end{pmatrix},$$

$$U_3 = \begin{pmatrix} 1 & 0 & 0 & 0 \\ 0 & \sqrt{\frac{1-2ab}{2(1-a)b}} & 0 & -\sqrt{\frac{2b-1}{2(1-a)b}} \\ 0 & 0 & 1 & 0 \\ 0 & \sqrt{\frac{2b-1}{2(1-a)b}} & 0 & \sqrt{\frac{1-2ab}{2(1-a)b}} \end{pmatrix},$$

$$U_4 = \begin{pmatrix} 1 & 0 & 0 & 0 \\ 0 & \sqrt{\frac{1-2ab}{2(1-a)(1-b)}} & -\sqrt{\frac{(2a-1)(2b-1)}{2(1-a)(1-b)}} & 0 \\ 0 & \sqrt{\frac{(2a-1)(2b-1)}{2(1-a)(1-b)}} & \sqrt{\frac{1-2ab}{2(1-a)(1-b)}} & 0 \\ 0 & 0 & 0 & 1 \end{pmatrix}.$$

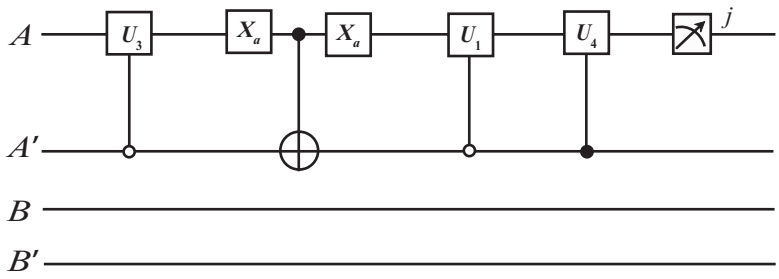

Fig. 2. Quantum circuit realizing the DEC by the direct sum extension method. Particle A is a four-level 'qudit' with logical states $\{|i\rangle, i = 0, 1, 2, 3\}$, and all others are qubits. The open (closed) circle indicates the conditioning on the qubit or qudit being set to zero (one).

Finally, Alice and Bob succeed in obtaining an EPR pair by choosing two suitable particles when the measurement result j is 1, 2, or 4 according to Eq. (4). For example, when $j = 4$ their choice is A' and B. For $j = 3$, Bob needs to measure either of his particles, say particle B, on the basis $|+\rangle = (|0\rangle_B + |1\rangle_B)/\sqrt{2}$, $|-\rangle = (|0\rangle_B - |1\rangle_B)/\sqrt{2}$ to obtain $|+\rangle$ or $|-\rangle$. Meanwhile, the particles A' and B' collapse into $(|00\rangle_{A'B'} + |11\rangle_{A'B'})/\sqrt{2}$ or $(|00\rangle_{A'B'} - |11\rangle_{A'B'})/\sqrt{2}$ to form an EPR pair. As has been noted, the entanglement concentration is always successful with unit success probability, no matter what the measurement result is. In particular, the minimum additional dimensions are added based on the direct sum extension method. As a result, the quantum circuit described here is simpler and easier to be realized in actual physical systems compared with that presented in Ref. [26]. Additionally, instead of using two extra dimensions of particle A, the protocol also can be constructed through the introduction of one ancillary qubit based on the tensor product extension method, but there will be more operations between two particles in its quantum circuits than that in Fig. 2. This means the direct sum extension method used here is more convenient when its physical realization is considered, especially in optical systems, which can be seen in the next section.

3 Optical realization scheme of DEC

In the following section, we propose a detailed physical scheme for implementing the optimal DEC protocol mentioned above via linear optical systems with the cavity-assisted interaction. The DEC protocol only requires the design of a scheme for the realization of U and orthogonal measurement, the quantum circuit of which is described in Fig. 2.

We first redefine the basis states introduced to fit actual optical systems. Because the quantum states of photons can be encoded into either their polarization or paths, we shall let the two states $|0\rangle$, $|1\rangle$ denote respectively the horizontal and vertical polarization of photons, and hereby rename them as $|H\rangle$ and $|V\rangle$. For instance, the initial state $|\Psi_0\rangle_{AA'BB'}$ can be expressed as $\left(\sqrt{a}\,|HH\rangle_{AB} + \sqrt{1-a}\,|VV\rangle_{AB}\right) \otimes \left(\sqrt{b}\,|HH\rangle_{A'B'} + \sqrt{1-b}\,|VV\rangle_{A'B'}\right)$. In the expanded space $\tilde{H}_A$, different paths (named T, S or R) are used to identify distinct states of photon A. For example, we encode $\left\{\left|HR^i\right\rangle, i = 0, 1, 2, 3\right\}$ as four levels of qudit A, which means photon A is in path R^i with the horizontal polarization.

Through the direct sum extension method, we now introduce a new entangled state with $\left\{\left|HS^i\right\rangle, i = 1, 2, 3, 4\right\}$ as quantum basis states of photon A, named path-polarization entan-

glement state. The state can be expressed as

$$\begin{aligned}|\Psi_S\rangle_{AAA'BB'} &= \sqrt{ab}\,|HS^1HHH\rangle + \sqrt{a(1-b)}\,|HS^2VHV\rangle \\ &\quad +\sqrt{(1-a)b}\,|HS^3HVH\rangle + \sqrt{(1-a)(1-b)}\,|HS^4VVV\rangle\,, \end{aligned} \tag{6}$$

where the particles are arranged in the order of $AAA'BB'$.

The state (6) is prepared by applying a unitary operation E on the initial state $|\Psi_0\rangle_{AA'BB'}$ in Eq. (1), as $E\,|\Psi_0\rangle_{AA'BB'} = |\Psi_S\rangle_{AAA'BB'}$. This can be achieved by using the cavity and linear optical devices in real experiment. The schematic setup is shown in Fig. 3, and the detailed implementation process can be seen as the two steps. First, the state $|H\rangle$ ($|V\rangle$) of photon A is converted into the basis state $|HT^2\rangle$ ($|HT^4\rangle$) of the expanded space by using a polarization beamsplitter and a polarization rotator, the function of which is to divide the photon A into the path T^2 (T^4) and flip the polarization of photon A in the path T^4 from vertical to horizontal, respectively. The state $|\Psi_1\rangle_{AAA'BB'}$ obtained here can be expressed as $\left(\sqrt{a}\,|HT^2H\rangle_{AAB} + \sqrt{1-a}\,|HT^4V\rangle_{AAB}\right) \otimes \left(\sqrt{b}\,|HH\rangle_{A'B'} + \sqrt{1-b}\,|VV\rangle_{A'B'}\right)$. In the second step, the state $|\Psi_1\rangle_{AAA'BB'}$ is continuously converted into $|\Psi_S\rangle_{AAA'BB'}$ by dividing photon A into four different paths S^i ($i = 1, 2, 3, 4$), whereby it can be seen that these paths are in one-to-one correspondence with the four initial basis states in Eq. (1). As a result, this makes it possible to execute controlled gates for two photons using single photon gates.

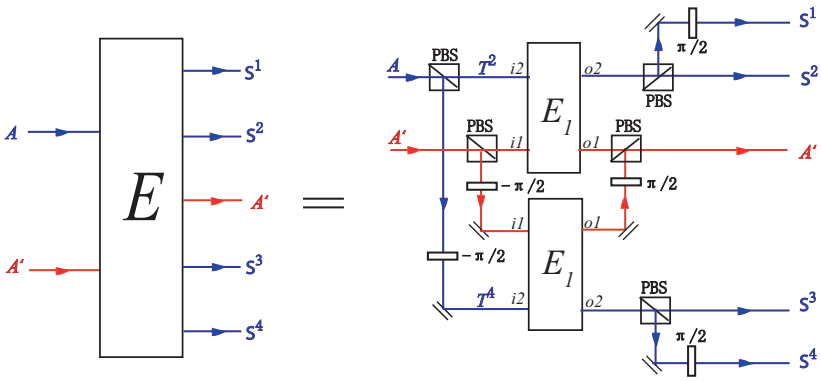

Fig. 3. Schematic setup of implementing operation E. Two photons in entangled state $|\Psi_0\rangle_{AA'BB'}$ enter gate E from left. Photon A can exit from the right side with four possible paths S^i ($i = 1, 2, 3, 4$) and A' exits through the remaining outlet path. The polarization beamsplitters (PBS) transmit photons in the $|H\rangle$ state, while reflect photons in the $|V\rangle$ state. The angles of the polarization rotators are either $-\pi/2$ or $\pi/2$.

The operation E_1 can be realized using either the nonlinear sign shift (NS) gate proposed by Knill, Laflamme, and Milburn [34, 35] or the controlled quantum phase-flip (CPF) gate proposed by Duan et al. [36]. We choose the latter gate because when compared with the first gate, the latter one is deterministic and does not need single-photon detectors with high efficiency. The schematic setup is shown in Fig. 4. The purpose of E_1 is to change the state of the photon entering via i_2 from $|H\rangle$ ($|V\rangle$) to $-|V\rangle$ ($-|H\rangle$), if the state of the photon via i_1 is $|H\rangle$. In all other cases, there is no state change.

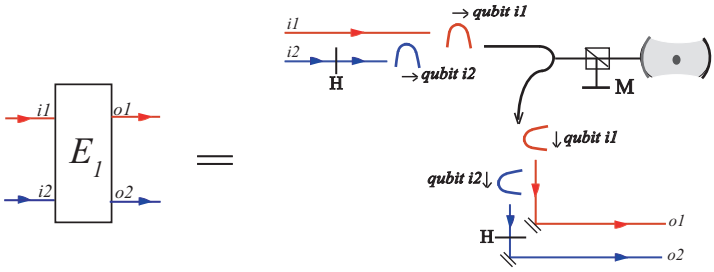

Fig. 4. Schematic setup of implementing operation E_1. It has two Hadamard gates H and one CPF gate implemented by the cavity-assisted interaction. The operation process of the optical cavity is the same as in Ref. [36].

The path-polarization entanglement state $|\Psi_S\rangle_{AA'BB'}$ undergoes the following four state evolutions to implement the operations described by the quantum circuit in Fig. 2.

$$\begin{aligned}
\sqrt{ab}\,|HS^1HHH\rangle \;\rightarrow\; & \frac{1}{\sqrt{2}}(\sqrt{2a(1-b)}\,|HR^0\rangle + \sqrt{(2a-1)(2b-1)}\,|HR^2\rangle \\
& +\sqrt{2b-1}\,|HR^3\rangle)\,|HHH\rangle\,, \qquad (7)\\
\sqrt{a(1-b)}\,|HS^2VHV\rangle \;\rightarrow\; & \sqrt{a(1-b)}\,|HR^0VHV\rangle\,, \qquad (8)\\
\sqrt{(1-a)b}\,|HS^3HVH\rangle \;\rightarrow\; & \frac{1}{\sqrt{2}}(\sqrt{1-2ab}\,|HR^1H\rangle + \sqrt{2b-1}\,|HR^3V\rangle)\,|VH\rangle\,, \qquad (9)\\
\sqrt{(1-a)(1-b)}|HS^4VVV\rangle \;\rightarrow\; & \frac{1}{\sqrt{2}}(\sqrt{1-2ab}\,|HR^1\rangle + \sqrt{(2a-1)(2b-1)}\,|HR^2\rangle)\,|VVV\rangle\,. \qquad (10)
\end{aligned}$$

The third evolution in Eq. (9) corresponds to the first two controlled gates in Fig. 2, and evolutions (7) and (10) correspond to the two remaining controlled gates. Here, the particles are arranged in the order $AA'BB'$. $\{|HR^i\rangle, i=0,1,2,3\}$ are four levels of qudit A.

These four evolutions are carried out as follows. Firstly, equations (7), (9) and (10), corresponding to controlled gates U_1, U_3, and U_4 of the quantum circuits in Fig. 2, are executed by polarized rotation gates θ_i $(i=1,2,3,4)$ of single photon A in paths S^1, S^3, and S^4, respectively. Meanwhile the remaining controlled gate (C-NOT gate), corresponding to Eq. (9), is executed by the interaction E_1 between two photons A and A', as shown in Fig. 5. The resultant states of these operations will divide photon A into the sub-paths $R^i_k (k=1,2)$; the optical length of paths R^i_1 and R^i_2 must be equal so as to make sure they can be re-combined into paths R^i by the single-photon interference [37]. For example, the process related with R^0 is expressed as

$$\begin{aligned}
& \sqrt{a(1-b)}\,|HR^0_1HHH\rangle + \sqrt{a(1-b)}\,|HR^0_2VHV\rangle \\
\rightarrow\; & \sqrt{a(1-b)}\,|HR^0H\rangle_{AAB}\,(|HH\rangle_{A'B'} + |VV\rangle_{A'B'})\,. \qquad (11)
\end{aligned}$$

And the results correspond to state $|\Psi_m\rangle_{AA'BB'}$in Eq. (2). It is worth noting that a minus symbol appears in path R^3. It is easy to verify that this has no impact on the realization of the protocol.

Finally, the states in Eq. (4) are achieved after photon A is detected in different paths R^i. Results obtained from the four detectors $D_i (i = 1, 2, 3, 4)$ correspond to $j = 1, 2, 3, 4$, respectively. The complete optical schematic setup for implementing the DEC protocol is shown as Fig. 5.

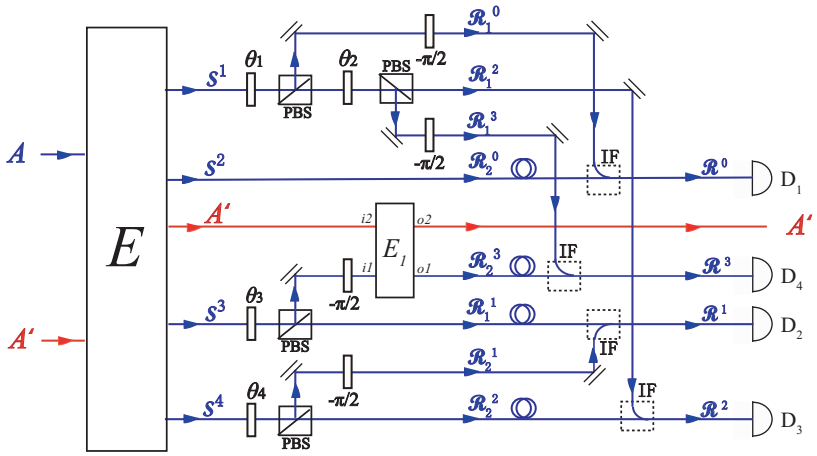

Fig. 5. Optical schematic setup for implementation of DEC protocol. Within dashed boxes IF, the sub-paths are re-combined by the single-photon interference. Angles of polarization rotators $\theta_i (i = 1, 2, 3, 4)$ are defined as $\sin(\theta_1) = \sqrt{(1-b)/b}$, $\tan(\theta_2) = \sqrt{1/(2a-1)}$, $\tan(\theta_3) = \sqrt{(2b-1)/(1-2ab)}$, $\cot(\theta_4) = \sqrt{(2a-1)(2b-1)/(1-2ab)}$.

It is noteworthy that only three elementary CPF gates are needed in the above scheme to implement the operations described by the quantum circuit in Fig. 2, which contains more than seven C-NOT gates that can be shown easily. This simplification should be attributed to the usage of the path-polarization entanglement state, which is obtained based on the direct sum extension method. This makes the controlled unitary operations with photon A as the target qudit implemented by performing single photon polarization rotations on A, thus further reducing the number of the controlled unitary operations between two photons to three. That is difficult to be achieved using the tensor product extension method. So, this scheme is easy to be implemented from an experimental point of view.

Since the controlled quantum phase flip gate is robust to practical noise and experimental imperfections in current cavity-QED setups (the cavity decay rate κ, the spontaneous emission rate γ_s of the atom, and the coupling rate g are typically $(\kappa, \gamma_s)/2\pi \approx (8, 5.2)$ and $g/2\pi \approx 25MHz$) [36], and the phase stability in single-photon interference can be guaranteed by keeping corresponding path lengths of the photon stable at subwavelength levels [37], the scheme is possible to be realized in an actual experiment. Especially, for the photon losses due to detector inefficiencies, numerical analysis made in section 4.1 shows that the single-photon detectors nowadays are good enough to have negligible impact on the viability of the scheme. Furthermore, the precision required by the detectors in this scheme is low as they are only used to distinguish between the vacuum and nonvacuum Fock number states.

4 Analysis and discussion

4.1 Discussion of success probabilities with imperfect detectors

In the section, we will study the impact of imperfect detectors on the probability of successfully realizing the DEC scheme. Here, photon loss and dark counts need to be considered when the photons are registered by the detectors. Using the distribution models in Ref. [35], we can calculate the success probabilities $P_i = ps_i/pd_i$, where $i = 1, 2, 3, 4$ correspond to the four measurement results ($j = 1, 2, 3, 4$) of photon A. ps_i represents the probability that the operation of the DEC scheme will succeed and the detectors will correctly detect the ith measurement result. pd_i represents the probability that the detectors report that the ith measurement result is obtained and the corresponding operation has succeeded, but in fact they may have failed.

Through the numerical simulation, we obtain the relationship between success probabilities $P_i, (i = 1, 2, 3, 4)$ and the parameters (η, g) of the imperfect detectors, shown in Fig. 6, in the case that $a = 0.51$, $b = 1/\sqrt{2}$. It can be seen that the success probabilities are higher than 99% if the single photon quantum efficiency η is more than 50% and the dark count probability g is lower than 10^{-4} for each detector.

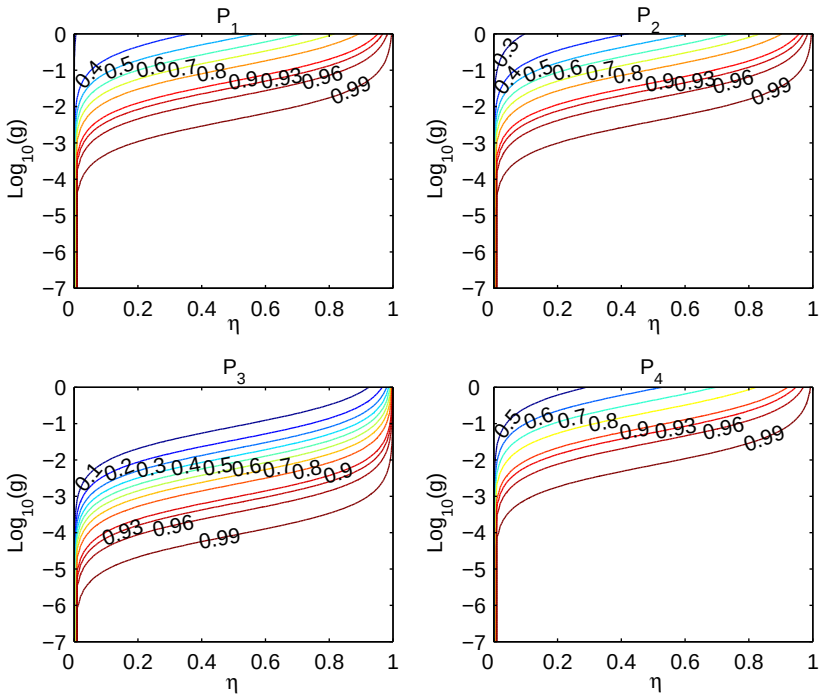

Fig. 6. The contour charts of success probabilities plotted as a function of the dark count probability g in logarithmic coordinate and the quantum efficiency η. The success probabilities $P_i, (i = 1, 2, 3, 4)$ correspond respectively to the four measurement results ($j = 1, 2, 3, 4$) of photon A. The height labels in the contour charts represent different levels of success probabilities.

According to a recent report [38], the quantum efficiency η and the dark count probability g

of a type of photon number detector are 73.8% and 1.1×10^{-6}, respectively. By assuming that photon A is detected by this kind of detectors, we ran a numerical simulation of the scheme, and manage to obtain the failed probabilities pf_i ($pf_i = 1 - P_i, i = 1, 2, 3, 4$) as a function of a and b, shown below in Fig. 7. We found that the success probability $P_i, (i = 1, 2, 3, 4)$ is higher than 99.5% when a and b satisfies the following conditions $0.505 \leq a \leq b \leq 0.999$ and $ab \leq 0.499$. On the other hand, when a and b satisfy $0.5 < a \leq b < 0.505$ ($0.499 < ab \leq 0.5$), P_3 (P_2) will sometimes be lower than 90%. This, however, does not affect the successful realization of the scheme since ps_3 (ps_2) is nearly equal to 0 in that case according to Eq. (5), i.e. the photon A is almost never detected by D_3 (D_2) as it virtually almost never takes route R_2 (R_1).

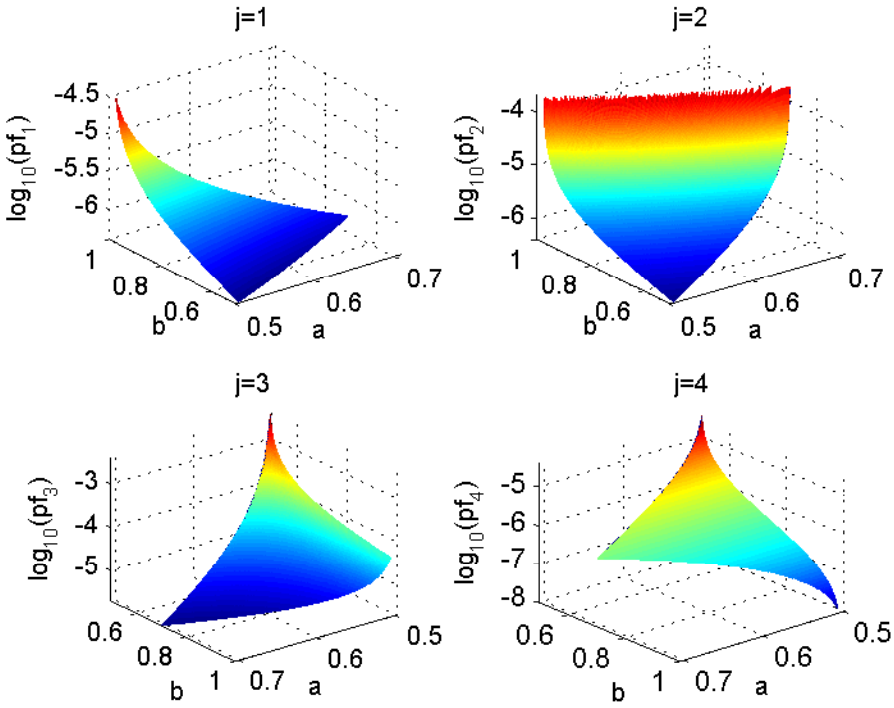

Fig. 7. The failed probabilities with imperfect detectors in logarithmic coordinate plotted as a function of a and b. The quantum efficiency η and the dark count probability g are 73.8% and 1.1×10^{-6} , respectively. a and b satisfy the conditions $0.505 \leq a \leq b \leq 0.999$ and $ab \leq 0.499$.

4.2 Analysis of mixed states

We now illustrate an analysis of the performance of the DEC protocol for the mixed states by considering the following scenario. Suppose that Alice and Bob share two pairs of entangled photons. They know *a priori* that each pair is in the state $|\psi_a\rangle$ with probability p, and in the state $|\psi_b\rangle$ with probability $1 - p$, but they do not know which state each pair is in. In this

situation, the state of the photon pair can be described by

$$\rho_{10} = p\,|\psi_a\rangle\,\langle\psi_a| + (1-p)\,|\psi_b\rangle\,\langle\psi_b|\,, \tag{12}$$

where, $|\psi_a\rangle = \sqrt{a}\,|HH\rangle + \sqrt{1-a}\,|VV\rangle$, $|\psi_b\rangle = \sqrt{b}\,|HH\rangle + \sqrt{1-b}\,|VV\rangle$, $0 \le p \le 1$, $1/2 < a \le b < 1$, $ab \le 1/2$.

In order to use the DEC protocol, Alice and Bob have to assume that the first pair is in the state $|\psi_a\rangle$ and the second pair is in the state $|\psi_b\rangle$. After performing the DEC protocol on these two photon pairs, we obtain the final state

$$\rho_{1f}^{j} = p^2\,|\phi_{1j}\rangle\,\langle\phi_{1j}| + p\,(1-p)\,(|\phi_{2j}\rangle\,\langle\phi_{2j}| + |\phi_{3j}\rangle\,\langle\phi_{3j}|) + (1-p)^2\,|\phi_{4j}\rangle\,\langle\phi_{4j}|\,, \tag{13}$$

where, $|\phi_{ij}\rangle = \left(\sum_{k=1}^{8} u_{2j-1,k}S_{k,i}\,|HH\rangle + \sum_{k=1}^{8} u_{2j,k}S_{k,i}\,|VV\rangle\right)/N_j$, $(i,j=1,2,3,4)$; j here denotes the measurement results of the DEC protocol; $u_{2j,k}$ and $u_{2j-1,k}$ are the elements of the unitary matrix U in Eq. (3), and N_j is the normalization constant. The four columns of the matrix S correspond to the four states, $|S_1\rangle = |\psi_a\rangle\,|\psi_a\rangle \oplus |O\rangle$, $|S_2\rangle = |\psi_a\rangle\,|\psi_b\rangle \oplus |O\rangle$, $|S_3\rangle = |\psi_b\rangle\,|\psi_a\rangle \oplus |O\rangle$, $|S_4\rangle = |\psi_b\rangle\,|\psi_b\rangle \oplus |O\rangle$, $|O\rangle = [0\ 0\ 0\ 0]'$.

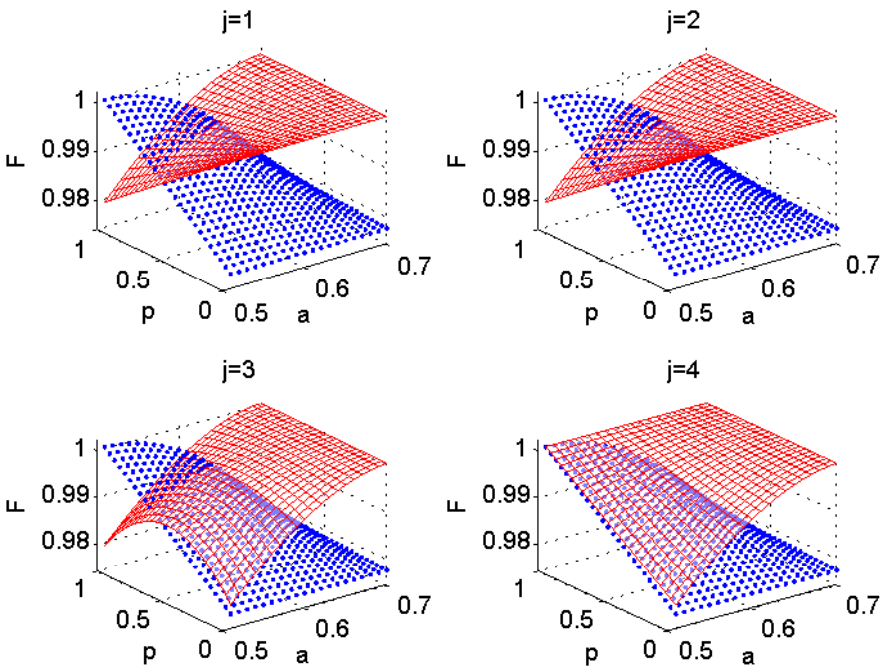

Fig. 8. The fidelities between the state $|E\rangle$ and the mixed states ρ_{10} and ρ_{1f}^{j}. During the calculation, b is set to $1/\sqrt{2}$. The fidelities about ρ_{10} and ρ_{1f}^{j} are represented by blue point arrays and red grids, respectively.

We then calculate the fidelities between the state $|E\rangle$ and the mixed states ρ_{10} and ρ_{1f}^{j}. Results are illustrated in Fig. 8. We can see that the DEC protocol is very effective when a

and p are close to $1/\sqrt{2}$ and 0 respectively. However, the effect is not good when a (p) is close to 0.5 (1), as the states ρ_{10} are very close to the maximally entangled state $|E\rangle$.

5 Conclusion

In summary, an optimal deterministic entanglement concentration protocol is proposed in this paper and its corresponding optical realization scheme is designed. The advantage of this protocol is illustrated not only from the fact that the ancillary dimensionality added and controlled operations needed are minimum, but also from the aspect that the quantum circuits built here are simpler than those in Ref. [26]. The optical realization scheme is designed following the evolution processes from the initial basis states to the final states. Based on the direct sum extension method, a path-polarization entanglement state is introduced to further reduce the number of controlled unitary operations between two photons. The simplification makes it sufficient to implement the protocol using only three CPF gates of two photons. The proposed scheme is possible to implement in experiment, and these strategies have critical applications for the design of the large-scale quantum computation and other quantum communication schemes. Finally, through the analysis of one kind of mixed states, it is verified that the DEC protocol is an effective way of recovering highly entangled pairs from some mixed states.

Acknowledgements

This work was supported by the National Natural Science Foundation of China (Grant No. 60677044, 11005099) and by the Fundamental Research Funds for the central universities (Grant No. 201013037).

References

1. A. K. Ekert (1991), *Quantum cryptography based on Bell's theorem*, Phys. Rev. Lett. 67, pp. 661-663.
2. C. H. Bennett, G. Brassard, C. Crepeau, R. Jozsa, A. Peres, and W. K. Wootters (1993), *Teleporting an unknown quantum state via dual classical and Einstein-Podolsky-Rosen channels* , Phys. Rev. Lett. 70, pp. 1895-1899.
3. D. Bouwmeester, J.W. Pan, K. Mattle, M. Eibl, H. Weinfurter, A. Zeilinger (1997), *Experimental quantum teleportation*, Nature 390, pp. 575-579.
4. A. Furusawa, J. L. Sørensen, S. L. Braunstein, C. A. Fuchs, H. J. Kimble, and E. S. Polzik (1998), *Unconditional Quantum Teleportation*, Science 282, pp. 706-709.
5. D. Gottesman and I. L. Chuang (1999), *Demonstrating the viability of universal quantum computation using teleportation and single-qubit operations*, Nature 402, pp. 390-393.
6. C. H. Bennett, H. J. Bernstein, S. Popescu, and B. Schumacher (1996), *Concentrating partial entanglement by local operations*, Phys. Rev. A 53, pp. 2046-2052.
7. S. Bose, V. Vedral, and P. L. Knight (1999), *Purification via entanglement swapping and conserved entanglement*, Pys. Rev. A 60, pp. 194-197.
8. H. K. Lo and S. Popescu (2001), *Concentrating Entanglement by Local Actions: Beyond Mean Values*, Phys. Rev. A, 63, 022301.
9. X. B. Wang and H. Fan (2003), *Entanglement concentration by ordinary linear optical devices without postselection*, Phys. Rev. A 68, 060302.
10. J. Watrous (2004), *Many copies may be required for entanglement distillation.* Phys. Rev. Lett, 93, 010502.

11. B. Groisman, N. Linden, and S. Popescu (2005), *Entanglement concentration of three-partite states*, Phys. Rev. A 72, 062322.
12. C. D. Ogden, M. Paternostro, and M. S. Kim (2007), *Concentration and purification of entanglement for qubit systems with ancillary cavity fields*, Phys. Rev. A. 75, 042325.
13. Y. B. Sheng, F. G. Deng, and H. Y. Zhou (2008), *Nonlocal entanglement concentration scheme for partially entangled multipartite systems with nonlinear optics*, Phys. Rev. A. 77, 062325.
14. D. Ballester (2009), *Entanglement accumulation, retrieval, and concentration in cavity QED*, Phys. Rev. A. 79, 062317.
15. A. J. Short (2009), *No Deterministic Purification for Two Copies of a Noisy Entangled State*, Phys. Rev. Lett. 102, 180502.
16. Y. B. Sheng and F. G. Deng (2010), *Deterministic entanglement purification and complete nonlocal Bell-state analysis with hyperentanglement*, Phys. Rev. A 81, 032307.
17. P. G. Kwiat, S. Barraza-Lopez, A. Stefanov, N. Gisin (2001), *Experimental entanglement distillation and 'hidden' non-locality*, Nature 409, pp. 1014-1017.
18. T. Yamomoto, M. Koashi, S. K. Ozdemir, and N. Imoto (2003), *Experimental extraction of an entangled photon pair from two identically decohered pairs*, Nature 421, pp. 343-346.
19. T. Yamamoto, M. Koashi, and N.Imoto (2001), *Concentration and purification scheme for two partially entangled photon pairs*, Phys. Rev. A 64, 012304.
20. Z. Zhao, T. Yang, Y. A. Chen, A. N. Zhang, and J. W. Pan (2003), *Experimental Realization of Entanglement Concentration and a Quantum Repeater*, Phys. Rev. Lett. 90, 207901.
21. R. Reichle, D. Leibfried, E. Knill, J. Britton, R. B. Blakestad, J. D. Jost, C. Langer, R. Ozeri, S. Seidelin, D. J. Wineland (2006), *Experimental purification of two-atom entanglement*, Nature 443, pp. 838-841.
22. R. Dong, M. Lassen, J. Heersink, C. Marquardt, R. Filip, G. Leuchs, U. L. Andersen (2008), *Experimental entanglement distillation of mesoscopic quantum states*, Nature Physics 4, pp. 919-923.
23. B. Hage, A. Samblowski, J. DiGuglielmo, A. Franzen, J. Fiurášek, R. Schnabel (2008), *Preparation of distilled and purified continuous-variable entangled states*, Nature Physics 4, pp. 915-918.
24. H. Takahashi, J. S. Neergaard-Nielsen, M. Takeuchi, M. Takeoka, K. Hayasaka, A. Furusawa, M. Sasaki (2010), *Entanglement distillation from Gaussian input states*, Nature Photonics 4, pp. 178-181.
25. F. Morikoshi (2000), *Recovery of Entanglement Lost in Entanglement Manipulation*, Phys. Re. Lett. 84, pp. 3189-3192; F. Morikoshi and M. Koashi (2001), *Deterministic entanglement concentration.* Phys. Rev. A. 64, 022316.
26. Y. J. Gu, W. D. Li, and G. C. Guo (2006), *Protocol and quantum circuits for realizing deterministic entanglement concentration*, Phys. Rev. A. 73, 022321.
27. H. F. Wang, S. Zhang (2009), *Scheme for Realizing Deterministic Entanglement Concentration with Atoms Via Cavity QED*, Int. J. Theor. Phys, 48, pp. 1678-1687.
28. P. X. Chen, J. A. Bergou, S. Y. Zhu and G. C. Guo (2007), *Ancilla dimensions needed to carry out positive-operator-valued measurement*, Phys. Rev. A 76, 060303.
29. J. Preskill, *Lecture Notes for Physics 229: Quantum Information and Computation*, http://theory.caltech.edu/ preskill/ph229/.
30. A. G. White, D. F. V. James, P. H. Eberhard, and P. G. Kwiat (1999), *Nonmaximally Entangled States: Production, Characterization, and Utilization*, Phys. Rev. Lett. 83, pp. 3103-3107.
31. M. A. Nielsen (1999), *Conditions for a Class of Entanglement Transformations*, Phys. Rev. Lett. 83, pp. 436-439.
32. A. Peres (1993), *Quantum Theory: Concepts and Methods* (Kluwer Academic, Dordrecht).
33. M. A. Neumark (1940), *Spectral functions of a symmetric operator*, Izv. Akad. Nauk SSSR Ser. Mat., 4:3, pp.277-318.
34. E. Knill, R. Laflamme, and G. Milburn (2001), *A scheme for efficient quantum computation with linear optics*, Nature 409, pp. 46-52.
35. S. Glancy, J.M. LoSecco, H.M. Vasconcelos, and C. E. Tanner (2002), *Imperfect detectors in linear*

optical quantum computers, Phys. Rev. A 65, 062317.
36. L. M. Duan and H. J. Kimble (2004), *Scalable Photonic Quantum Computation through Cavity-Assisted Interactions*, Phys. Rev. Lett. 92, 127902.
37. H. Wei, W. L. Yang, Z. J. Deng, and M. Feng (2008), *Many-qubit network employing cavity QED in a decoherence-free subspace*, Phys. Rev. A 78, 014304.
38. O. Thomas, Z. L. Yuan, J. F. Dynes, A. W. Sharpe, and A. J. Shields (2010), *Efficient photon number detection with silicon avalanche photodiodes*, Phys. Rev. Lett. 97, 031102.